

Mitigation of Inter-cell Interference in an Industrial Communication Network by Coordinated Scheduling

JACK BENNHAGEN AND STEFAN MILANOVIC

MASTER'S THESIS

DEPARTMENT OF ELECTRICAL AND INFORMATION TECHNOLOGY

FACULTY OF ENGINEERING | LTH | LUND UNIVERSITY



Mitigation of Inter-cell Interference in an Industrial Communication Network by Coordinated Scheduling

Jack Bennhagen and Stefan Milanovic
elt15jb1@student.lu.se, elt15smi@student.lu.se

Department of Electrical and Information Technology
Lund University

Supervisors:
Harsh Tataria, Lund University
Emma Wittenmark, Ericsson AB
Oskar Drugge, Ericsson AB

Examiner:
Fredrik Rusek, Lund University

June 24, 2020

© 2020
Printed in Sweden
Tryckeriet i E-huset, Lund

Abstract

With Industry 4.0, the manufacturing industries are transitioning from wired to wireless communication between machines which put high demands on the network system. This can be achieved with the fifth generation (5G) of wireless communication by utilizing two fundamental key features in New Radio (NR), Massive Machine-Type Communication (mMTC) and Ultra-Reliable Low Latency Communication (URLLC). To handle the increased network load that comes with mMTC, multiple cells may need to be implemented, which introduces Inter-Cell Interference (ICI) to the network system. The added ICI may reduce the overall performance of the system.

The aim of this thesis was to investigate if the number of devices could be increased while maintaining a high reliability. The objective was to mitigate uplink ICI by coordinating schedulers between two cells in an industrial communication network. The coordination feature was implemented in an already existing Ericsson AB simulator. The approach was to identify devices that contributed more to the ICI by using the Reference Signal Received Power (RSRP) measurement. These devices were then allocated frequency resources in a protected frequency band which restricted the other cell from allocating on the same frequency resources in the same uplink slot.

The results showed that by coordinating the schedulers between two cells, a 10 % increase in the number of devices could be achieved while upholding a reliability of 99.9 %.

Popular Science Summary

Increasing the number of devices in a wireless network by optimizing the use of frequency resources

The Fifth Generation (5G) of wireless communication is enabling manufacturing industries to transition from wired to wireless communication. This allows a reliable low latency communication between machines which is a keystone in the next industrial revolution, called Industry 4.0. This will increase the number of connected devices in the wireless network. In this thesis a method for increasing the capacity in the network to support an increased number of devices by 10% is presented.

In contrast to mobile broadband where high data rates are important, the industry has other requirements such as low latency and a high reliability. These requirements mean that the transmitted data need to arrive at the designated destination within a set time limit, very often. The requirements must still be met even when the number of devices in the network are increasing. Since the amount of resources available in a network is finite, it limits the increase of devices in the network.

One way to be able to increase the number of devices is to add another cell to the network. This will increase the resources which will allow more devices to communicate in the network. A drawback with introducing another cell is the increased interference. This type of interference, Inter-Cell Interference

(ICI) will limit the capacity, in terms of number of devices in the network. In this thesis the aim was to see if the capacity could be increased by mitigating the ICI.

The frequency spectrum is divided in time and frequency resources that are used for data transmission. In a two-cell deployment the frequency resources are duplicated and can be used in both cells simultaneously. However, due to ICI this does not implicate that the capacity can be doubled. A proposed method in this thesis is to select a number of frequency resources that are not allowed to be reused in the other cell. This means that a part of the frequency spectrum will be restricted from being used in the other cell. Devices that are using the resources in the restricted area will not be exposed to ICI since no other devices

will be using these resources.

By testing the proposed method in a simulated industrial scenario, the theoretical result showed that the capacity

in the network could be increased by up to 10 % while maintaining a high reliability.

Acknowledgements

We would like to start off by thanking Ericsson AB in Lund for giving us the opportunity to conduct this thesis, as well as for providing us with all the tools needed. Furthermore, we would like to express our gratitude to our supervisors at Ericsson, Emma Wittenmark and Oskar Drugge, who have invested their time and shared their knowledge with us throughout the thesis. Without their guidance this thesis would be impossible to conduct. We would also like to thank Harsh Tataria, our supervisor at Lund University, for his invaluable feedback and advice along the way.

Finally we are forever grateful for the support both of our families have shown us during the time of our studies.

Sincerely,
Jack Bennhagen
Stefan Milanovic

Table of Contents

| | | |
|----------|---|-----------|
| 1 | Introduction | 1 |
| 1.1 | Disposition | 1 |
| 2 | Background | 3 |
| 2.1 | Numerology | 3 |
| 2.2 | Duplexing Configuration | 4 |
| 2.3 | Orthogonal Frequency-Division Multiplexing (OFDM) | 5 |
| 2.4 | Physical Channels | 5 |
| 2.5 | Physical Resource Block | 5 |
| 2.6 | Signal-to-Interference-plus-Noise Ratio (SINR) | 8 |
| 2.7 | Link Adaptation (LA) | 8 |
| 2.8 | Reference Signal Received Power (RSRP) | 9 |
| 2.9 | Inter-cell Interference | 10 |
| 2.10 | Power Control | 11 |
| 2.11 | Scheduling | 11 |
| 3 | Previous Work and Model Assumptions | 13 |
| 3.1 | Introduction | 13 |
| 3.2 | Network Deployment | 13 |
| 3.3 | Frame Structure | 15 |
| 3.4 | Data Traffic | 15 |
| 3.5 | Requirements | 15 |
| 3.6 | Capacity | 18 |
| 4 | Method and Results | 21 |
| 4.1 | Simulation | 21 |
| 4.2 | Baseline | 21 |
| 4.3 | The Static Coordination Method, First Iteration | 21 |
| 4.4 | The Static Coordination Method, Second Iteration | 29 |
| 4.5 | The Dynamic Approach | 34 |
| 5 | Discussion and Conclusion | 37 |
| 5.1 | Static Coordination Method | 37 |
| 5.2 | Dynamic Coordination Method | 38 |

| | |
|---|-----------|
| 5.3 Conclusion | 38 |
| References _____ | 39 |
| A UE Locations _____ | 41 |
| B Utilization of PRB Grid For Baseline _____ | 45 |
| C PRB Allocation For CC-UE _____ | 47 |
| D Data Traffic Arrival Pattern _____ | 49 |

List of Figures

| | | |
|------|---|----|
| 2.1 | The different numerologies in 5G-systems. | 3 |
| 2.2 | Different duplex configurations. FDD (left) compared to TDD (right). | 4 |
| 2.3 | PRB grid, over one slot, for 30 kHz SCS, assuming 250 PRBs. | 7 |
| 2.4 | The added margin to SINR estimation. | 9 |
| 2.5 | Illustration of how ICI occurs. | 10 |
| 3.1 | Factory environment with blockers [18]. | 14 |
| 3.2 | DL:UL = 3:1 slot format. | 15 |
| 3.3 | Data arrival traffic, equally spaced over the traffic period. | 15 |
| 3.4 | Best case scenario vs. worst case scenario. | 17 |
| 3.5 | DL outage probability for different network loads where the dashed lines show the requirements limits not to exceed [18]. | 19 |
| 3.6 | UL outage for different network loads where the dashed lines show the requirements limits not to exceed [18]. | 19 |
| 4.1 | Representation of the different areas in the PRB grid. | 23 |
| 4.2 | The location of 450 UEs, which cell they belong to and their classification. | 24 |
| 4.3 | Histogram of the number of CE-UE per UL slot in cell 0. | 26 |
| 4.4 | Histogram of the number of CE-UE per UL slot in cell 1. | 26 |
| 4.5 | Outage for different sizes of protected PRB areas. Values on x-axis are for cell 0, for cell 1 the values are 2 times larger. | 26 |
| 4.6 | Outage for CE-UE and CC-UE, for different network loads. | 28 |
| 4.7 | Mean and 99th percentile utilization of PRB Grid for different network loads. | 28 |
| 4.8 | Number of PRB allocated per uplink slot for CE-UE. | 29 |
| 4.9 | SINR for CC-UE with different network loads. From the first implementation of static coordination method. | 30 |
| 4.10 | SINR for CE-UE with different network loads. From the first implementation of static coordination method. | 30 |
| 4.11 | UL transmit power before power control modifications. | 31 |
| 4.12 | UL transmit power after power control modifications. | 31 |
| 4.13 | UL SINR for CE-UE. | 32 |
| 4.14 | The highest and mean number of PRB allocated for CE-UE. | 32 |

| | | |
|------|--|----|
| 4.15 | UL outage with power control modifications. | 33 |
| 4.16 | Outage for the worst case user with dynamic allocation. | 35 |
| 4.17 | Utilization of PRB grid for different network loads with dynamic allocation. | 35 |
| 4.18 | Comparison of outage for worst case UEs for dynamic approach and baseline. | 36 |
| A.1 | UE locations for a network load of 100 UEs. | 41 |
| A.2 | UE locations for a network load of 200 UEs. | 41 |
| A.3 | UE locations for a network load of 300 UEs. | 42 |
| A.4 | UE locations for a network load of 400 UEs. | 42 |
| A.5 | UE locations for a network load of 450 UEs. | 43 |
| A.6 | UE locations for a network load of 500 UEs. | 43 |
| A.7 | UE locations for a network load of 550 UEs. | 43 |
| B.1 | Utilization of PRB grid for different network loads with no coordination (baseline). | 45 |
| C.1 | Mean and worst case PRB allocation for CC-UEs at a network load of 550 UEs. | 47 |
| D.1 | Data traffic arrival pattern for 20 uplink slots. | 49 |

List of Tables

| | | |
|-----|---|----|
| 2.1 | Maximum number of resource blocks (N_{RB}) for different bandwidths and numerologies. | 6 |
| 2.2 | The different numerologies, μ_i , and the SCS spacings. | 7 |
| 3.1 | Parameters for the simulation. | 16 |
| 4.1 | Number of CE-UE in percentage for a network load of 450 UEs. | 24 |
| 4.2 | Parameters for static allocation method, first iteration. | 25 |
| 4.3 | Parameters for static allocation method, second iteration. | 33 |
| 4.4 | Parameters for dynamic allocation method. | 34 |

List of Abbreviations and Acronyms

3GPP Third Generation Partnership Project

4G Fourth Generation

5G Fifth Generation

BLER Block Error Rate

CC-UE Cell Center User Equipment

CE-UE Cell Edge User Equipment

CP Cyclic Prefix

CQI Channel Quality Information

CRC Cyclic Redundancy Check

CRS Cell-specific Reference Signal

CSI Channel State Information

DL Downlink

DMRS Demodulation Reference Signal

FDD Frequency Division Duplex

FEC Forward Error Correction

FIFO First-In First-Out

gNB gNodeB

ICI Inter-Cell Interference

InH Indoor Hotspot

ISI Inter-Symbol Interference

LA Link Adaptation

LDPC Low Density Parity Check

LTE Long Term Evolution

MAC Medium Access Control
MTC Machine Type Communication
mMTC Massive Machine Type Communication
MRC Maximal-Ratio Combining
NR New Radio
OFDM Orthogonal Frequency-Division Multiplexing
PDU Protocol Data Unit
PRB Physical Resource Block
PUCCH Physical Uplink Control Channel
PUSCH Physical Uplink Shared Channel
RSRP Reference Signal Received Power
SC Subcarrier
SCS Subcarrier Spacing
SINR Signal-to-Interference-plus-Noise Ratio
SNR Signal-to-Noise-Ratio
SR Scheduling Request
SS Synchronization Symbol
TDD Time Division Duplex
TTI Transmission-Time Interval
UCI Uplink Control Information
UE User Equipment
UL Uplink
URLLC Ultra-Reliable Low Latency Communication

Introduction

Development of fifth-generation (5G) wireless communication systems are enabling the next industrial revolution, known as Industry 4.0 [1]. With a 5G cellular network, devices are able to directly communicate with each other over the wireless medium. For the manufacturing industry, this brings a new way of thinking when designing a manufacturing plant. Removing the need for cables makes the production more agile and thus reduces the cost [2]. In industrial scenarios, Ultra-Reliable Low-Latency Communication (URLLC) is the key component to be able to achieve reliable Machine-Type Communication (MTC) [3].

This thesis is a continuation of a study conducted by Ericsson AB where a wireless industrial environment was simulated and the relations between capacity, latency bound, reliability for multi-cell deployments were evaluated. The purpose for this master thesis was to investigate if the capacity, i.e the total number of devices that can be served, given the same network setup and scenario, could be increased further while still maintaining the reliability in terms of successful transmissions within the latency bound. The proposed research method in this thesis was to coordinate schedulers between cells and thereby mitigate the inter-cell interference. The implementation of the coordination was done by altering the already implemented wireless network scenario.

1.1 Disposition

Chapter 2 gives a theoretical background for subjects relevant to this thesis. The model assumptions and the previous work conducted by Ericsson Research is further elaborated in Chapter 3. The method for conducting the thesis is described in Chapter 4 together with the results. In chapter 5 the results from the previous chapter are discussed. Chapter 5 also summarizes the thesis with conclusions and further studies are proposed.

This chapter details theoretical concepts to bestow the reader a general understanding of the technical features used in the thesis.

2.1 Numerology

The frame structure of NR systems involve mixed numerologies, and hence the ability to handle a variety of subframe configurations. To this end, it is different than that of Fourth-Generation (4G) Long-Term Evolution (LTE) systems. This allows NR to be more flexible relative to its predecessors. Both in NR and in LTE, a frame is 10 ms in total and is built up by 10 subframes where each subframe is 1 ms. Since the subcarrier spacing (SCS) in LTE is fixed at 15 kHz, a subframe consists of two slots. The definition of a subcarrier will be described in detail below. One of the differences from LTE is that in NR, different SCS can be used, ranging from 15 kHz to 240 kHz [4]. In NR, the length of a slot changes with different SCS, but a slot is always 14 symbols long. Figure 2.1 shows the variation of slot timings with increasing sub-carrier spacing.

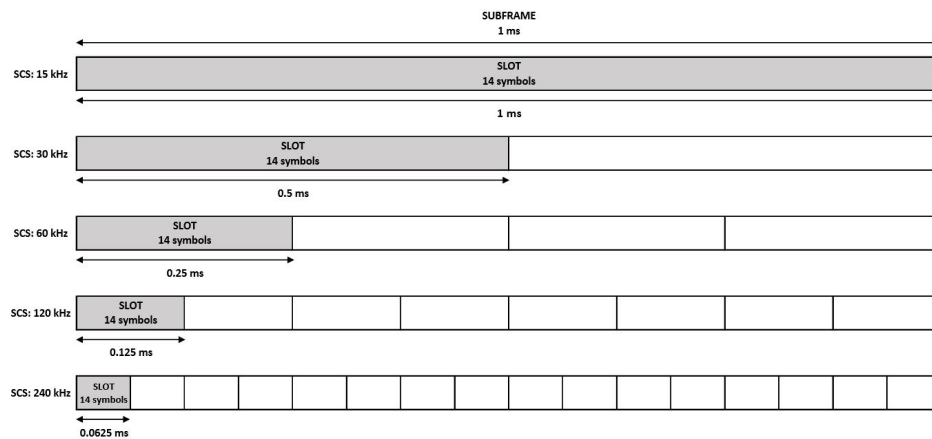


Figure 2.1: The different numerologies in 5G-systems.

The different numerologies are one of the main technology components in NR that are needed to achieve URLLC [5]. With a larger SCS, more OFDM-symbols can be transmitted during a subframe as can be seen in Figure 2.1. The different frame structures can shorten the duration of the Transmission-Time Interval (TTI). From a URLLC perspective a shorter TTI is an advantage.

The reliability aspect of URLLC is defined as the rate of successful packet transmissions, with the definition that a packet is successful if it is received correctly within the stipulated latency bound. With a higher reliability, more packets will be transmitted successfully within the latency requirement. The reliability requirements varies with different deployments and use cases. In NR, release 16, reliability as high as 99.9999% is hoped to be achieved [7].

2.2 Duplexing Configuration

There are two types of duplexing configurations, Time-Division Duplex (TDD) and Frequency-Division Duplex (FDD). To be able to use TDD or FDD, the spectrum has to be unpaired and paired, respectively. In higher frequencies, it is more common for spectrum to be unpaired, this is one reason that TDD is more common [16]. In FDD, the spectrum is divided in two separate frequency bands, one for DL and one for UL. UL and DL transmission can be done simultaneously as can be seen to the left in Figure 2.2. However, the paired band, which is needed for FDD duplexing, is often a licensed band which makes it more expensive than an unpaired band. An issue with licensed bands is that the bands are not always available and aggregating multiple carriers introduce extra constraints on the radio access network hardware utilized, making it an unprofitable exercise the vast majority of the time. Another drawback is the guard band that is needed between UL and DL frequency regions. The guard band is used to avoid cross-link interference and this spectrum becomes wasted since it can not be used for traffic.

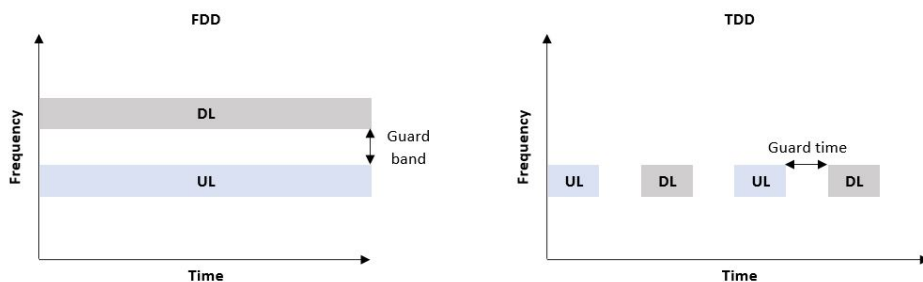


Figure 2.2: Different duplex configurations. FDD (left) compared to TDD (right).

In TDD, UL and DL transmissions are transmitted on the same frequency band, but are divided in time. Figure 2.2 (right) shows how UL and DL are divided in time, on the same frequency. An advantage with TDD over FDD is that a UE is not required to be able to receive and transmit on two different frequency bands simultaneously, which minimizes the constraint on the UE. A drawback with TDD

is that UL and DL transmissions can not be done simultaneously since the time slots are dedicated for either UL or DL transmissions. This can contribute to an added latency, where the amount of added latency depends on the chosen frame structure. With the flexibility of NR the latency can be reduced by using the different available numerologies.

2.3 Orthogonal Frequency-Division Multiplexing (OFDM)

Orthogonal Frequency-Division Multiplexing (OFDM) is well known for being robust to time dispersion. The waveform is used in both LTE and NR [4]. An OFDM-symbol consists of multiple subcarriers which are closely spaced and orthogonal to each other. Each subcarrier carries one symbol, where the number of bits per symbol varies depending on the modulation scheme. Link adaptation (LA) in turn varies the modulation scheme depending on the SINR, such that a target error rate (e.g. block error rate (BLER)) can be reached. LA will be explained later on. The modulation schemes and SINR will be explained below. By distributing the bits in frequency, multiple subcarriers can be transmitted within the same signal. This is due to the subcarriers being orthogonal to each other. Since the OFDM-symbols are closely spaced in time, they become prone to multipath propagation which may cause Inter-Symbol Interference (ISI) from the previous OFDM-symbol. To avoid ISI a cyclic prefix (CP) is used. The last part of an OFDM-symbol is copied and added to the start of the same OFDM-symbol. The drawback with the addition of a cyclic prefix is that it reduces the spectrum efficiency and the data rates.

2.4 Physical Channels

The physical channels are the channels closest to the actual transmission of data and the channels are being transmitted over the radio interface. The physical channels used in this thesis are not optical fibre, copper-wire, air etc. The expression is used as by 3GPP in an abstract sense when describing what type of transmission is done. The two channels used in this thesis will be Physical Uplink Shared Channel (PUSCH) and Physical Uplink Control Channel (PUCCH). PUSCH is used to transmit UEs data and PUCCH is used to send control data to the gNB.

2.5 Physical Resource Block

The resource grid models the structure of transmitted signal, where the smallest physical resource in NR is called a resource element. A resource element is seen as one subcarrier in one OFDM-symbol. A resource block is defined by 12 subcarriers [11, p.14]. In NR, resource blocks are only defined in the frequency domain, however in LTE, a resource block is also defined in the time domain. A resource block in LTE is defined as 12 subcarriers, or 12 resource elements, and 14 OFDM-symbols. This is because, in LTE, a subframe is always defined as two slots where

each subframe contains 14 OFDM-symbols due to only having one numerology [4, p.109]. In NR, a slot always consists of 14 OFDM-symbols, however the number of slots per subframe varies depending on the chosen numerology. There are three types of resource blocks, common resource blocks, virtual resource blocks and Physical Resource Blocks (PRB) [4, p.111]. PRBs are used to describe the actual transmitted signal, i.e. which subcarriers, in terms of resource blocks, are available to send data on.

Table 2.1: Maximum number of resource blocks (N_{RB}) for different bandwidths and numerologies.

| | Bandwidth | SCS spacing | | |
|----------|-----------|-------------|--------|--------|
| | | 15 kHz | 30 kHz | 60 kHz |
| N_{RB} | 5 MHz | 25 | 11 | N/A |
| N_{RB} | 10 MHz | 52 | 24 | 11 |
| N_{RB} | 15 MHz | 79 | 38 | 18 |
| N_{RB} | 20 MHz | 106 | 51 | 24 |
| N_{RB} | 25 MHz | 133 | 65 | 31 |
| N_{RB} | 30 MHz | 160 | 78 | 38 |
| N_{RB} | 40 MHz | 216 | 106 | 51 |
| N_{RB} | 50 MHz | 270 | 133 | 65 |
| N_{RB} | 60 MHz | N/A | 162 | 79 |
| N_{RB} | 80 MHz | N/A | 217 | 107 |
| N_{RB} | 90 MHz | N/A | 245 | 121 |
| N_{RB} | 100 MHz | N/A | 273 | 135 |

The available time-frequency resources for the system can be represented by a resource grid consisting of PRBs. The height of the grid can be configured up to a maximum size which varies depending on the numerology. The maximum number of resource blocks depend on the bandwidth and numerology and can be seen in Table 2.1, which is standardized in NR in release 16 [6]. The width of the resource grid is determined by the number of OFDM-symbols within a subframe and, in 5G, it varies with the numerology as follows:

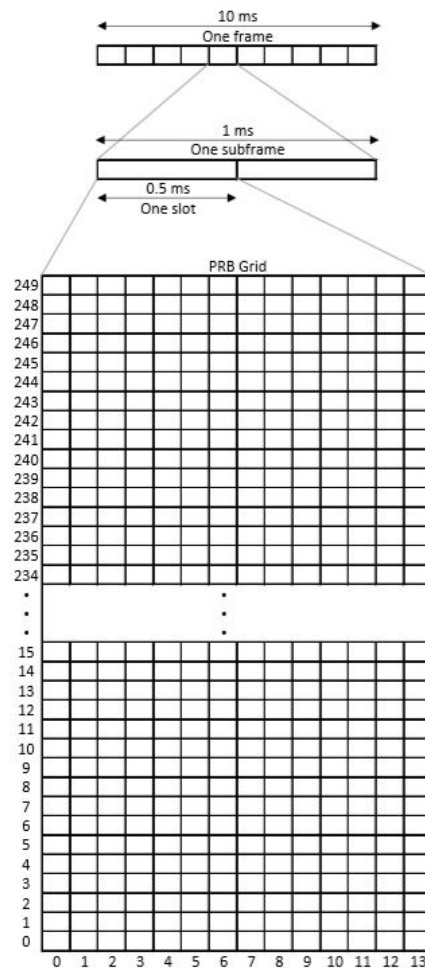
$$l = 14 \cdot 2^\mu \quad (2.1)$$

where l is the width and the OFDM-symbols are numbered from 0 to $l - 1$ and μ is the different numerologies as seen in Table 2.2. Figure 2.3 gives an overview of what the grid with 30 kHz SCS can look like.

As previously stated, a set of allocated PRBs are used for the actual transmitted data. When referring to how many resources that were used for a transmissions, it is common to use PRBs. In this thesis, the number of PRBs used for a transmission will be used as an evaluation metric for the implemented feature. In this thesis one PRB will be defined as 12 subcarriers and 14 OFDM-symbols since the transmissions are done per slot. Using the number of PRBs as a metric gives

Table 2.2: The different numerologies, μ , and the SCS spacings.

| μ | SCS spacing |
|-------|-------------|
| 0 | 15 kHz |
| 1 | 30 kHz |
| 2 | 60 kHz |
| 3 | 120 kHz |
| 4 | 240 kHz |

**Figure 2.3:** PRB grid, over one slot, for 30 kHz SCS, assuming 250 PRBs.

a good understanding of how much bandwidth is left to transmit on and if full transmission capacity has been reached or not. The number of PRBs needed for a transmission depends on the size of the data that is required to be sent, given the Signal-to-Interference-plus-Noise-Ratio (SINR).

2.6 Signal-to-Interference-plus-Noise Ratio (SINR)

SINR, or Signal-to-Noise-Ratio (SNR) with the interference calculations included, takes into account multiple factors describing the reception quality and the throughput that can be achieved in a network system. SINR is defined as in equation (2.2) where P is the transmit power, G is the path gain which is determined by the path loss, fading and shadowing caused by buildings or obstructions. N is the noise which is assumed to be generated within the receiver. The interference, I , can be caused by simultaneous transmissions in a network system [9].

$$SINR = \frac{P \cdot G}{I + N} \quad (2.2)$$

One particular case where interference might occur is in a multi-cell deployment scenario where the same spectrum is shared between two or more cells. Transmissions can take place on the same frequency resources in both of the cells. When two UEs in two different cells are transmitting on the same PRBs simultaneously might cause interference at the gNB receivers since the receiving end will pick up both the wanted signals as well as the interfering signal from a UE in a neighbouring cell. Inter-Cell Interference (ICI) will be explained in section 2.9.

SINR is calculated and used by Link Adaptation (LA), which will be explained further in the following subsection, when allocating a sufficient number of PRBs, so that a successful transmission can be achieved. With a higher SINR, the network is more reliable, and a higher throughput, in terms of data bits per second, can be supported.

2.7 Link Adaptation (LA)

LA is a term used with allocation process and it determines what modulation scheme and code rate should be used, given the estimated SINR, so that a sufficient number of PRBs would be allocated for the UE.

Modulation

The modulation scheme affects the number of bits that can be used per subcarrier. More bits per subcarrier means that more data bits can be sent during a time slot. The supported modulation schemes in 5G, release 15, are QPSK, 16QAM, 64QAM and 256QAM [10] which gives 2, 4, 6 and 8 bits per subcarrier, respectively. With a higher SINR, higher modulation can be used.

Coding

LA also determines an appropriate code rate when doing Forward Error Correction (FEC) coding. With FEC coding, redundant bits are added to the actual data bits to try to prevent errors in data transmissions. Two types of coding schemes are available in 5G, release 15, Low Density Parity Check (LDPC) coding and polar coding [11]. For the data channels in UL, i.e. PUSCH, LDPC is used while polar coding is used for the control channel PUCCH. The code rate is defined as the ratio between actual data bits and the total number of bits in a transmission.

LA Margin

Before a transmission, LA is estimating SINR. An SINR estimation error might occur due to the current channel conditions being estimated on previous transmissions. One way to try and mitigate the estimation error is by adding a margin on the estimation of SINR. The margin can be seen in Figure 2.4.

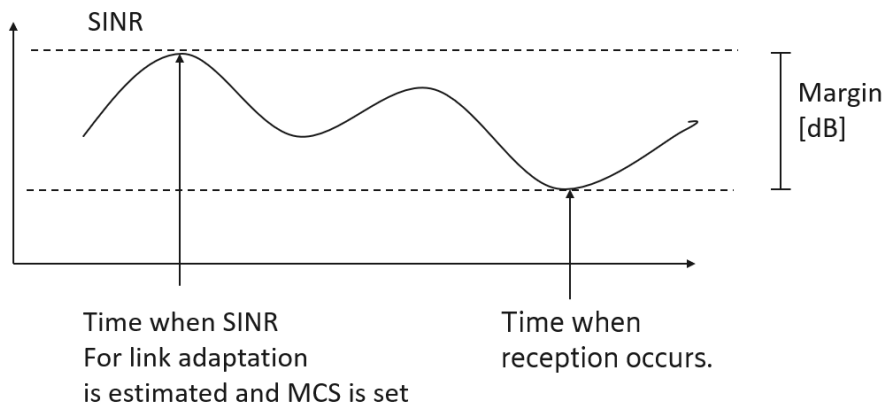


Figure 2.4: The added margin to SINR estimation.

In conclusion, the number of PRBs needed for a successful transmission is determined by LA and depends on the SINR and the amount of data that needs to be sent. With a higher SINR, higher modulation schemes and code rates can be used, decreasing the number of PRBs needed for the UE to transmit its data. With a lower SINR, lower modulation schemes and code rates need to be used, increasing the total number of PRBs allocated to a UE.

2.8 Reference Signal Received Power (RSRP)

RSRP measurement indicates the signal strength from the gNB to a UE. The gNB transmits reference signals to the UE, the UE then evaluates the received power of the received signals and reports back the received power to the gNB. This information is needed when performing e.g. cell selection, cell reselection

or handover for a UE. In LTE, the RSRP measurement is based on Cell-specific Reference Signal (CRS), however in NR, this is now done on Synchronization Signal (SS) or Channel State Information (CSI) reference signals. SS-RSRP is defined as the linear average over the power contributions (in [W]) of the resource elements that carry secondary SS [12]. CSI-RSRP is defined as the linear average over the power contributions (in [W]) of the resource elements that carry CSI reference signals configured for RSRP measurements within the considered measurement frequency bandwidth in the configured CSI-RS occasions [12].

2.9 Inter-cell Interference

When a UE is transmitting to the gNB in the cell it belongs to, the signal may also be picked up by other gNBs. The gNB in a neighbouring cell may receive the transmitted signal which affect the reception of signals aimed for that gNB. This unwanted transmission to the neighbouring cell will cause Inter-cell Interference (ICI). If the neighbouring cells are sharing frequency spectrum the ICI can lower the performance in the cells. A lowered SINR due to increased interference might trigger the power control to increase the UEs transmit power which then will increase the ICI in the neighbouring cell.

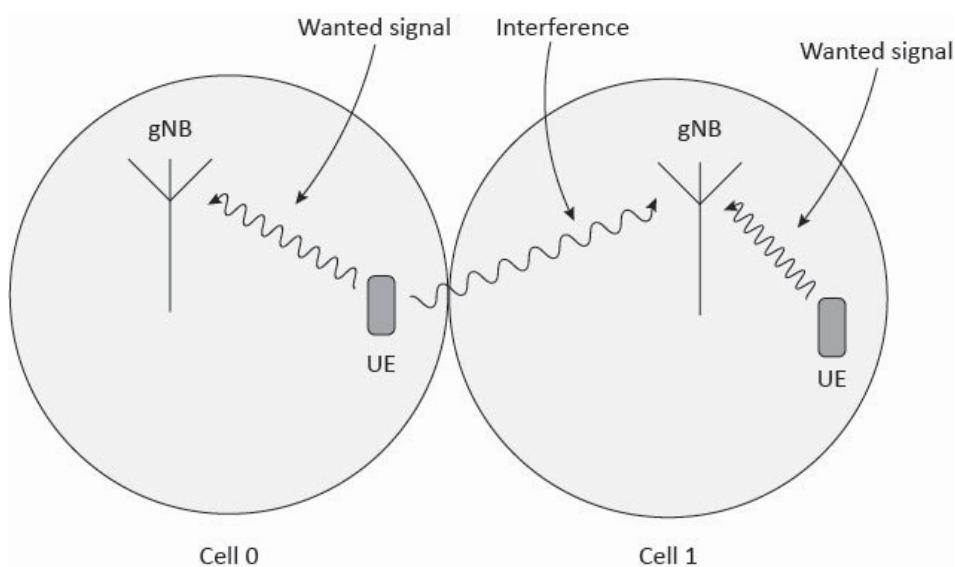


Figure 2.5: Illustration of how ICI occurs.

The SINR is estimated per PRB using an assumption of an Maximal-Ratio Combining (MRC) receiver and based on previous transmissions. The interference estimates per antenna are calculated based on DMRS and filtered using a moving average filter across a certain number of previous transmissions.

2.10 Power Control

Power control is used to adjust the transmit power of a UE such that the transmitted signal can be correctly decoded at the gNB. It is also responsible of reducing the ICI. There is a trade off that the power control need to handle as a higher transmit power would increase the SINR for a signal, however this would also increase the interference for other signals transmitted on the same frequency resources. The decisions made by the power control are based on a combination of Open-loop power control and Closed-loop power control. In Open-loop power control, measurements on DL transmissions are used for estimating the UL path loss and then transmit power is set according to the estimates. Closed-loop power control however utilize network measurements on previous UL transmissions to regulate the transmit power. Since a UE has a finite power limit the power control is required to compare the calculate transmit power against a maximum allowed transmit power. The calculation of transmit power per carrier

$$P_{PUSCH} = \min\{P_{Max}, P_0 + \alpha \cdot PL + 10 \cdot \log_{10}(2^\mu \cdot M_{RB}) + \Delta_{TF} + \delta\} \quad (2.3)$$

can be seen in the simplified Equation (2.3) [4, p.302] where:

- P_{PUSCH} is the UL transmit power.
- P_{max} is the allowed maximum transmit power per carrier.
- P_0 is the target received power.
- PL is the estimated UL path loss.
- α is related to the fractional path loss, which is configurable by the network.
- μ is related to the SCS.
- M_{RB} is the number of allocated resource block for the transmission.
- Δ_{TF} is related to the MCS.
- δ is the adjusted power due to the closed-loop power control.

The power control chooses the smallest of the two values in Equation (2.3) to ensure that the UE does not transmit above allowed transmission power per carrier.

2.11 Scheduling

The scheduler resides in the Medium Access Control (MAC) layer and is responsible for assigning time-frequency resources to a UE that either has data to receive in a DL slot or has data to send in an UL slot. DL and UL scheduling are both done in the gNB but can be done independently of each other. Only UL scheduling will be described, since the scope of this thesis is interference mitigation for UL transmissions.

2.11.1 Uplink Scheduling

The uplink scheduling process starts with a Scheduling Request (SR) that is sent from a UE. SR is sent when a UE has data to transmit to the gNB. SR can either be sent on the PUCCH or as Uplink Control Information (UCI) on the PUSCH.

The scheduler has a buffer where information regarding all UEs that have sent a scheduling request is stored. In what order the UEs are sorted in the buffer depends on the chosen scheduling configuration. Some of the well-known scheduling principles are Round Robin, First-In, First-Out (FIFO) queuing and proportionally fair. In this thesis the scheduling principle that will be used is delay based scheduling. The UEs are sorted according to their accumulated queuing delay, in ascending order.

When a UE is scheduled, it needs to be allocated PRBs to send data on. There are two main allocation strategies, random and sequential. With random allocation strategy the scheduler chooses the starting point for PRBs randomly and then continues the allocation incrementally in the PRB grid. A new randomly selected starting point is chosen for each UE. In the sequential allocation strategy, the starting point for the allocation is chosen at the first available PRB and then continues the allocation incrementally in the PRB grid. Before allocating time-frequency resources to the UE, the gNB needs to estimate an SINR. The estimation is based on the Demodulation Reference Signal (DMRS) from the UE, which is a part of every OFDM-symbol [4]. As previously stated, the number of PRBs required for a successful transmission is based on the SINR and the size of the data packets. The scheduler continues to schedule UEs that want to transmit until the buffer of scheduling requests is empty or until no more UEs can be allocated in the finite PRB grid. The scheduler then sends grants to the scheduled UEs, informing them when to transmit and on what PRBs.

Previous Work and Model Assumptions

This master thesis was proposed by Ericsson Research as a continuation of previous studies of wireless network performance in an industrial deployment. The traffic model, network scenario and basic assumptions were provided as a starting point. Ericsson is conducting research before a standard is set thus some parameters are chosen based on empirical studies and assumptions while other parameters are based on previous standards. To protect the confidentiality of Ericsson AB, some parameters cannot explicitly be explained.

3.1 Introduction

The purpose of the previous work was to evaluate the relations between capacity, latency bound, reliability and multi-cell deployments with a 10 ms latency requirement and a 99.9% reliability requirement in an industrial scenario. To evaluate the industrial network, two simulators were setup with parameters used in earlier studies conducted by Ericsson AB. Due to Ericsson's confidentiality the simulators will henceforth be referred to as *Simulator A* and *Simulator B*.

3.2 Network Deployment

The industrial environment will only be described briefly because the development of the industrial environment was not in the scope of the thesis. The propagation model that was used by simulator A was based on the 3GPP Indoor Hotspot (InH) with some modifications to suit the industrial scenario [14]. The modifications that were made to the InH model, to better suit the industrial scenario, are described by Joachim Sachs et al. in a conference paper [8]. The modifications can be summarized as:

- In the InH model LOS and NLOS links are distinguished by a stochastic probability model, however since it is assumed that there are not any walls in a typical industrial environment only LOS links will be expected.
- The modeling of metal sheets as blockers, were explicitly done according to a model from 3GPP, where the attenuation for each multi path component was calculated by a blockage model [14].

- The shadow fading was changed from 3 dB, as specified in the InH model, to 5 dB.
- The angular and delay spread were changed to closely match the measured data from the industrial scenarios.

The environment that was given from the simulator A can be seen in Figure 3.1. The deployment scenario modeled an industrial factory-like setting with the dimensions of 180 m x 90 m x 20 m (W x D x H). Metal sheets, blockers, of uniformly distributed width within the interval 3 to 10 m and height of 5 m were used to model the occurrence of e.g. mobile robots, machines and metal sheets that are usually present in manufacturing scenarios. The maximum number of UEs that were generated by simulator A was set to 1750, an arbitrarily chosen number. The data, the propagation analysis and environment, from simulator A was exported to a file which was imported into another simulator, simulator B. In simulator B, various parameters such as the number of UEs, duplex configurations etc. can be altered to suit the intended scenario and it is in simulator B that the majority of changes were made.

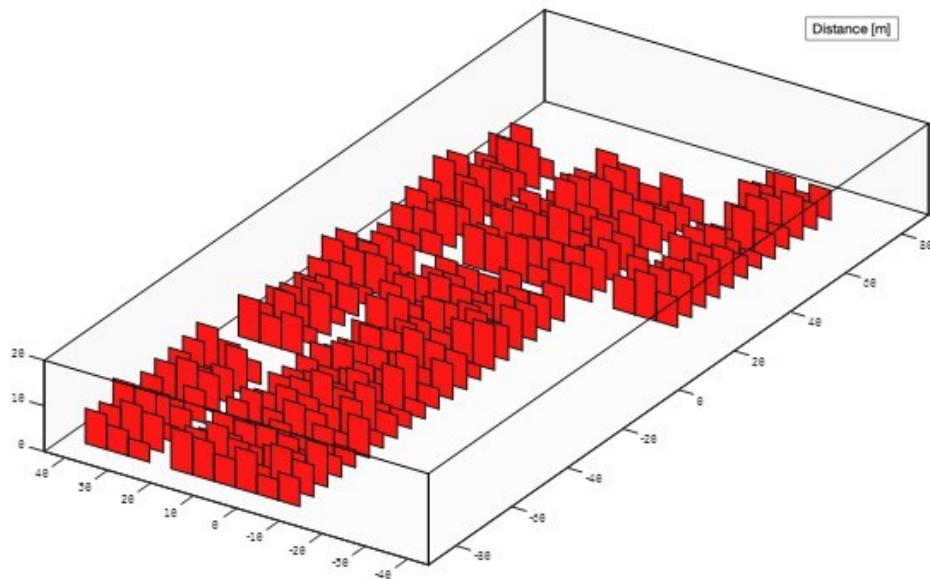


Figure 3.1: Factory environment with blockers [18].

Devices

The type of UEs that were modeled in the network system were latency-critical UEs with small Protocol Data Unit (PDU) to transmit.

3.3 Frame Structure

A TDD configuration was used with a three slots DL-frame and one slot UL-frame, DL:UL = 3:1 slot format as shown in Figure 3.2. This configuration was chosen to be used since this configuration is being used in existing industry 4.0 factories. To be able to implement a wireless system, the configuration needs to be chosen so it can co-exist with licensed deployments and adjacent bands in e.g. Sweden and Germany. The chosen numerology was 30 kHz SCS which gives a slot length of 0.5 ms. The 30 kHz SCS was chosen since this numerology is being used by existing Ericsson products[17]. The frequency band that was used in the simulation was 3.5-3.6 GHz which would give a bandwidth of 100 MHz. A 100 MHz bandwidth and a 30 kHz SCS would result in a maximum of 273 available PRBs, as shown in Table 2.1. However in the study, 250 PRBs were used, to align with previous work done at Ericsson AB.

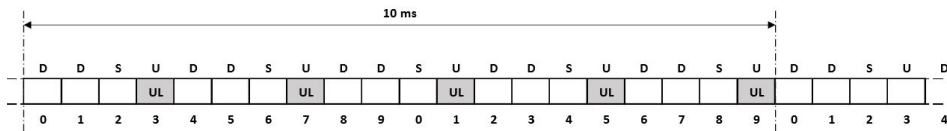


Figure 3.2: DL:UL = 3:1 slot format.

3.4 Data Traffic

The data traffic arrival pattern describes how the PDUs are sent from e.g. UE to gNB. The data arrival pattern used in this thesis is that the data arrives in an equally spaced manner over the traffic period and can be seen in Figure 3.3. The traffic period sets the latency requirement which will be described below.

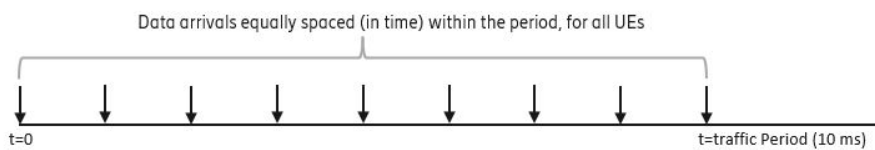


Figure 3.3: Data arrival traffic, equally spaced over the traffic period.

3.5 Requirements

A traffic model with a traffic arrival periodicity of 10 ms and with a PDU size of 115 bytes was investigated. The PDU size is selected to reflect communication of small control packets being transmitted. The PDU rate was based on use cases such as a mobile robot communication and a process monitoring, where a 10 ms

Table 3.1: Parameters for the simulation.

| | |
|--------------------------------|--|
| Numerology | 30 kHz SCS, 250 PRBs, 0.5 ms slot |
| PRB | 12 SC x 14 OFDM-symbols |
| PDU size | 115 bytes |
| System Bandwidth | 100 MHz |
| Carrier Frequency | 3.5 GHz |
| Antenna Model | gNB: 4 Rx and 4 Tx UE: 4 Rx and 1 Tx |
| Frame Structure | TDD (DDSU) |
| Scheduling Scheme | Dynamic Grant, Delay Based Priority |
| Scheduling Request Periodicity | 2 ms |
| UL Power Control SINR Target | 10 dB |
| LA Margin | 6 dB |
| UL SINR Estimation for LA | Maximum Ratio Combining (MRC) |
| Simulation Length | > 100000 packets per UE. 200 seeds each 6 seconds long. Each seed randomizes propagation fading pattern and packet arrival time within period. UE locations are fixed. |
| PUCCH Model | Error Free Reception, no LA |

PDU-rate can be expected [13]. It was tested if the latency requirement could be achieved with a reliability of 99.9%. The latency is defined as the time it takes for a PDU from when it reaches a higher application layer to when the PDU arrives at corresponding application layer at the receiver side. The latency requirement was defined to be equal to the PDU rate, i.e. a packet needs to be transmitted and received at the gNB before the next PDU packet arrives at the UE. PDUs that exceed the latency requirements were considered as outages.

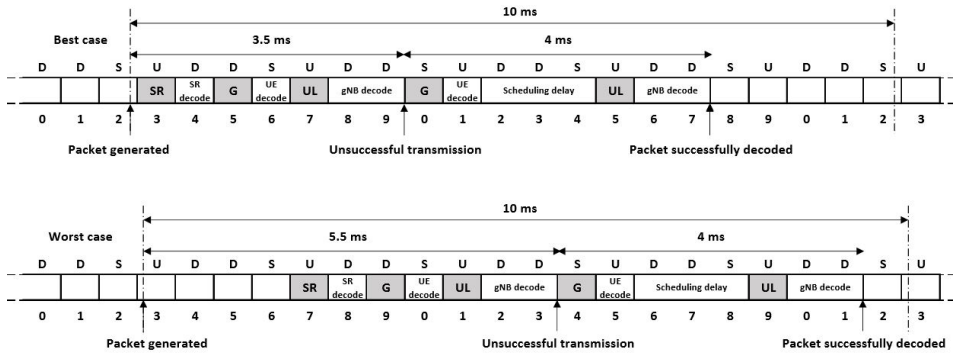


Figure 3.4: Best case scenario vs. worst case scenario.

With a 10 ms latency requirement, only one retransmission is possible. For a best case scenario, the data that needs to be transmitted arrives at a lower physical level before an UL slot, e.g. slot 2, as depicted in the upper part of Figure 3.4. This means that the UE can send its SR in the upcoming UL slot, slot 3, assuming zero processing time. The gNB decodes the SR in slot 4 and sends a grant to the UE in slot 5. The UE decodes the grant in slot 6 and sends the data in slot 7 and the message is decoded by the gNB in slot 8 and 9. This is an initial transmission, if successful, this would have taken approximately 3.5 ms. However, if the transmission were to be unsuccessful, a retransmission is needed, which means that the gNB has to send another grant to the UE in slot 0. The UE decodes the grant in slot 1 but has to wait until the next UL slot to transmit, which is 3 slots later. The UE transmits the message in slot 5, and the gNB decodes the message in slot 6 and 7. Together, the initial transmission and retransmission, took 7.5 ms. Since a retransmission takes 4 ms, another retransmission would result in an outage. The lower part of Figure 3.4 shows how long it would take for an initial transmission and a retransmission in a worst case scenario. The difference between the two cases is that in the worst case scenario, the data that needs to be transmitted arrives to the physical layer during an UL slot, slot 3 in the lower part of Figure 3.4. This means that the UE has to wait until next UL slot, slot 7, to send the SR. Due to the scheduling delay, it takes 2 ms more for an initial transmission compared to the best case scenario. The total time for an initial transmission and a retransmission for the worst case scenario is 9.5 ms, hence another retransmission would result in an outage.

3.6 Capacity

The outage probability for DL and UL, found in the previous work done at Ericsson, are depicted in 3.5 and 3.6, respectively. It can be seen that the capacity limit, with respect to the reliability requirement, for the UL transmissions is lower than for the DL transmissions. This means that the UL transmissions are the bottleneck in the network system where the capacity limit, for two cells, is reached at 400 UEs. The focus for this thesis will be on the UL, as this is the bottleneck of the system, in a two cell deployment.

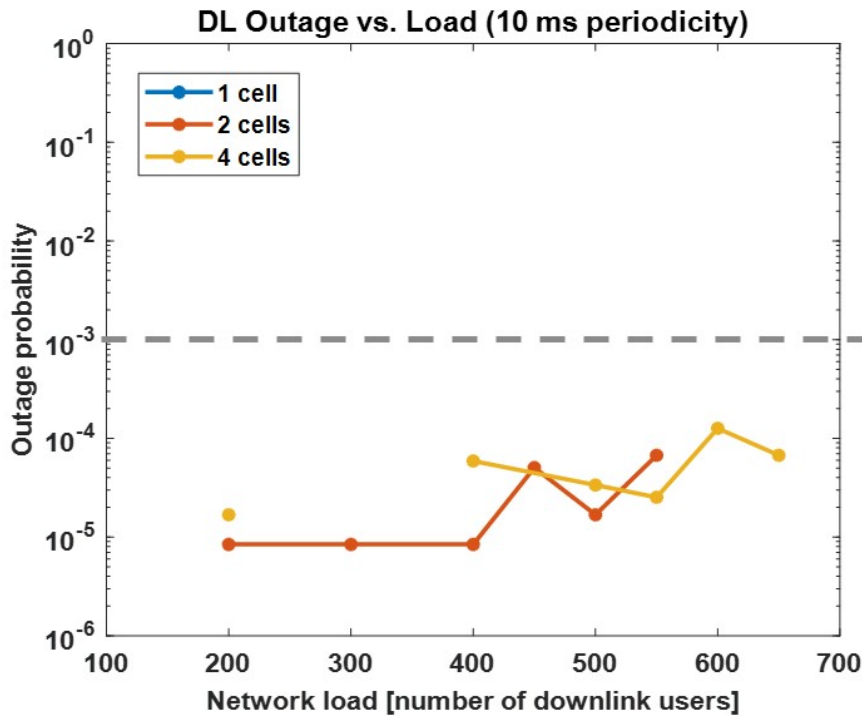


Figure 3.5: DL outage probability for different network loads where the dashed lines show the requirements limits not to exceed [18].

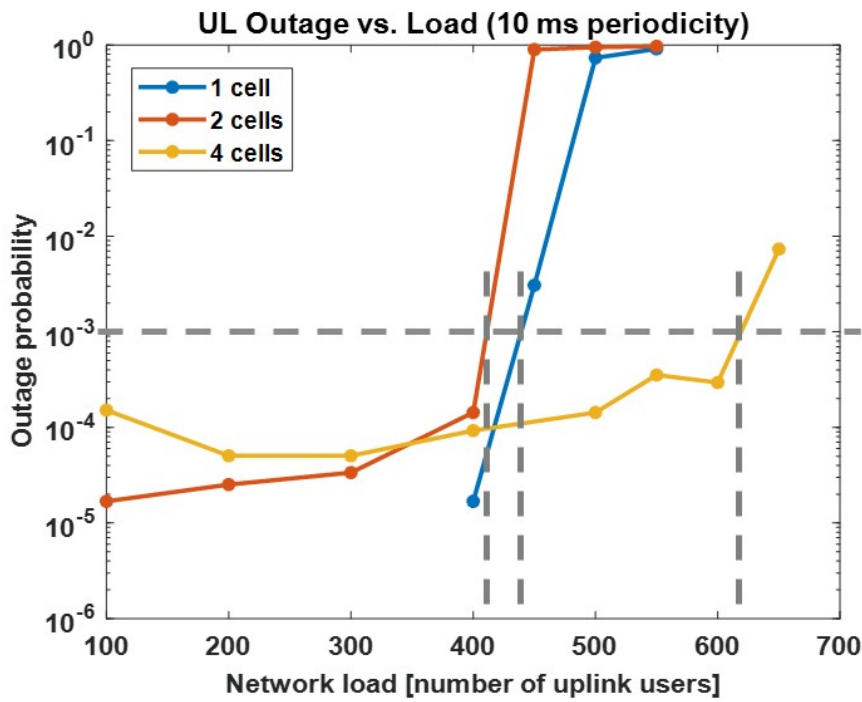


Figure 3.6: UL outage for different network loads where the dashed lines show the requirements limits not to exceed [18].

Method and Results

The task of implementing coordination of schedulers was divided into two subtasks, static coordination and dynamic coordination. In this chapter, the definition and implementation of the subtasks will be explained. The results will also be presented and explained in this section to give a better understanding of the assumptions made as the work progressed. Finally, the dynamic allocation will be compared to when no coordination was implemented in the schedulers, since this is the implementation goal in the thesis.

4.1 Simulation

The algorithms explained in the sections below were implemented in Simulator B. The simulator ran on 200 seeds for each implementation, where each seed simulated a time-span of 6 seconds. During the 6 seconds each UE transmitted over 100 000 packets. The data exported from Simulator B were post-processed and analysed in Matlab.

4.2 Baseline

During the implementations, it was found that a parameter had to be changed. The change of parameter value meant that the results from the implementations could not be compared with the previous work done by Ericsson, i.e. Figure 3.6. The parameter change was applied for all of the results presented in chapter 4. The scenario, without coordination of schedulers, was simulated with the parameter change. The results from the simulation will be compared to the results from the implemented methods.

4.3 The Static Coordination Method, First Iteration

The first task in the static approach was to identify UEs that contributed more to ICI, using a suitable method. After the UEs had been identified, they were given a part of the available frequency spectrum where they would be allocated PRBs to transmit on. This reserved part of the frequency spectrum would only be available by one cell, hence the transmission done in this part of the spectrum would not

be interfering the other cell. In the static coordination method, the reserved part of the frequency spectrum was kept constant for every UL slot.

Identification Method

The chosen method of identification was to use RSRP measurement. The idea was to compare RSRP measurements from the two cells to identify UEs that had similar signal strength to both cells. UEs identified by this method were labeled Cell Edge UEs (CE-UE), while the rest were labeled Cell Center UEs (CC-UE). The RSRP measurements were compared to each other as in equation (4.1)

$$T \leq |RSRP_0 - RSRP_1| \quad (4.1)$$

where T denotes the threshold, $RSRP_0$ and $RSRP_1$ are the RSRP measurements from cell 0 and cell 1, respectively. If the difference is less than or equal to a certain threshold, the UEs were classified as CE-UE. It was decided that the UEs only had to be classified during the initial cell selection. This resulted in that the total number of CE-UE remained constant during the entire simulation.

PRB Restrictions

With a two cell deployment, each cell was restricted from allocating PRBs on a certain frequency spectrum, i.e. the restricted area was reserved for the other cell. The purpose of restricting a frequency spectrum for a cell was to only allow CE-UEs in the other cell to transmit on. It is assumed that CE-UE below the threshold will need a high number of PRBs due to ICI. By implementing restricted areas, it is expected that the capacity will increase, since the number of allocated PRBs for CE-UE will be reduced. The restriction resulted in the PRB grid being divided into different areas.

The PRB grid was divided in the following sub-areas:

- PUCCH area: a common area for all UEs to transmit uplink control signals.
- CE-UE area: an area restricted to CE-UEs to transmit on. These frequency resources are not shared with the other cells.
- CC-UE common area: an area for CC-UE. Frequency resources are shared with the other cells.

With static coordination, the sizes of the restricted areas were fixed and did not change depending on the number of CE-UE per UL scheduling. The different sub-areas and the restrictions in the cells can be seen in figure 4.1.

Threshold

There is a correlation between the threshold and the number of CE-UE, as a larger threshold would enable more UEs to be classified as CE-UE. To choose an appropriate value for the threshold, the scenario was simulated with a network load of 450 users. This network load was chosen due to it not meeting the latency requirement as can be seen in Figure 3.6. The threshold was swept in the interval

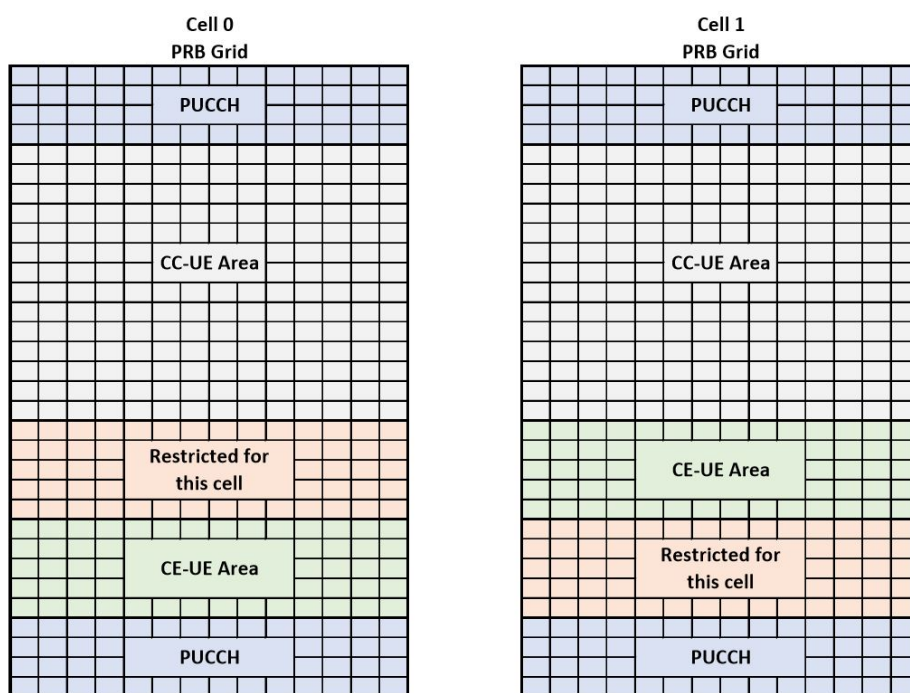


Figure 4.1: Representation of the different areas in the PRB grid.

from 2 to 10 dB with a step size of one. Table 4.1 shows the ratio of CE-UE v.s. total number of UEs for for the threshold sweep. It was arbitrarily chosen that the ratio should not exceed 10%, hence the threshold of 3 dB was chosen.

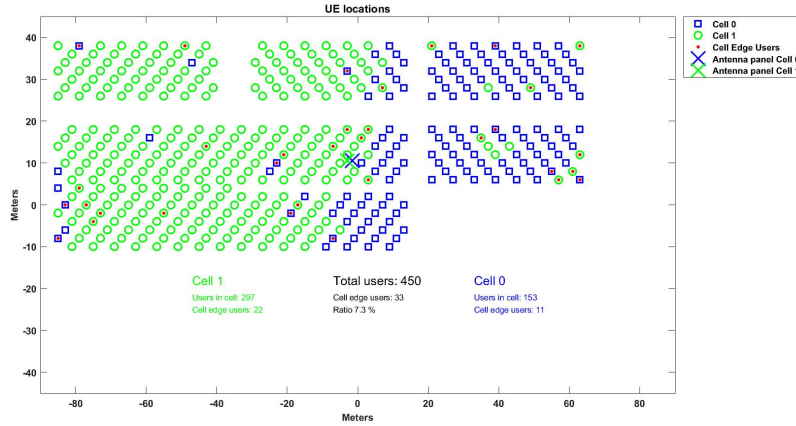


Figure 4.2: The location of 450 UEs, which cell they belong to and their classification.

Table 4.1: Number of CE-UE in percentage for a network load of 450 UEs.

| Threshold | Number of CE-UE |
|-----------|-----------------|
| 2 dB | 5.3 % |
| 3 dB | 7.3 % |
| 4 dB | 10.2 % |
| 5 dB | 12.7 % |
| 6 dB | 16.9 % |
| 7 dB | 20.7 % |
| 8 dB | 25.1 % |
| 9 dB | 30.9 % |
| 10 dB | 34.4 % |

Size of the Restrictions

With a threshold chosen, the number of PRBs per restricted areas could be determined. Since the PRBs in the restricted areas are restricted from being used by the other cell, the interference can be assumed to be negligible. With low interference, the LA would yield a high FEC coding and a high modulation format. The number of bits per PRB was calculated with equation 4.2 where B is bits, N_{SC} is

the number of subcarriers in a PRB, S is the number of OFDM-symbols available for transmission and M is the modulation.

$$B = N_{SC} \cdot S \cdot M \quad (4.2)$$

With 12 subcarriers, 12 OFDM-symbols available for transmission and a 64QAM modulation format, the maximum number of bits per PRB resulted in 864. With a PDU-size of 920 bits (115 bytes) and added bits due to LDPC coding, Cyclic Redundancy Check (CRC) checksum and different protocol overhead, 2 PRBs would be necessary.

Figure 4.2 depicts the location of the UEs in the industrial scenario. It can be seen that there are 11 CE-UE in cell 0 and 22 CE-UEs in cell 1. To get an understanding of how many CE-UEs that are scheduled per UL slot, the scenario was simulated. How many CE-UE were scheduled per UL slot, in each cell, were plotted in Figure 4.3 and Figure 4.4. The scenario was simulated again to determine the most optimal sizes for the restricted areas. The area size of the restricted areas were swept from 4 to 14 for cell 0 and 8 to 24 in cell 1. The sweep intervals were set according to the min and max values from the histograms, assuming that 2 PRBs were sufficient per CE-UE transmission. According to the outage plot, depicted in Figure 4.5, the most optimal sizes were 8 PRBs and 16 PRBs for cell 0 and cell 1, respectively.

Table 4.2: Parameters for static allocation method, first iteration.

| | |
|----------------------------------|---------|
| RSRP threshold | 3 dB |
| CE-UEs in cell 0 | 11 UEs |
| CE-UEs in cell 1 | 22 UEs |
| Size of protected area in cell 0 | 8 PRBs |
| Size of protected area in cell 1 | 16 PRBs |

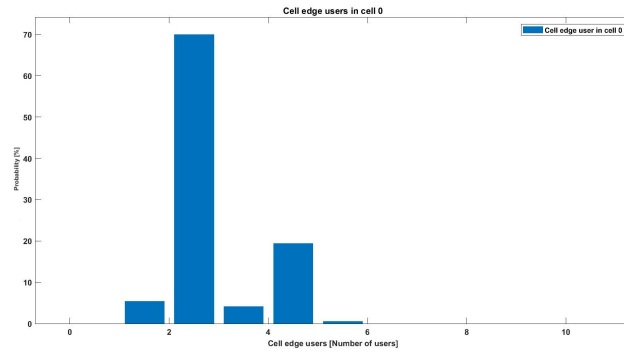


Figure 4.3: Histogram of the number of CE-UE per UL slot in cell 0.

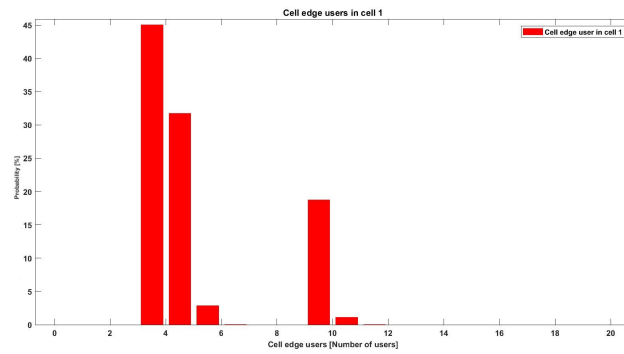


Figure 4.4: Histogram of the number of CE-UE per UL slot in cell 1.

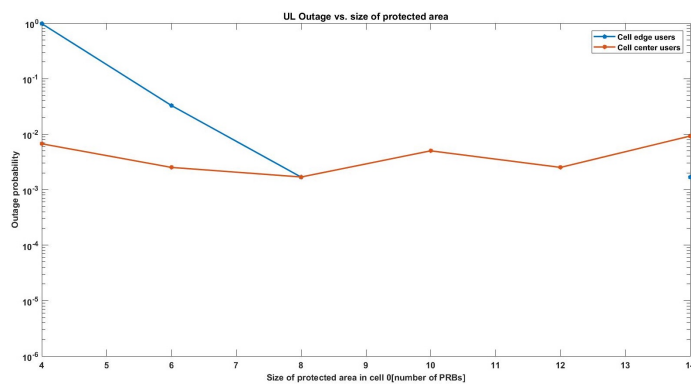


Figure 4.5: Outage for different sizes of protected PRB areas. Values on x-axis are for cell 0, for cell 1 the values are 2 times larger.

Allocation Procedure

With the parameters in Table 4.2, a static coordination scenario could be simulated. The UEs classification is used to set the area of the PRB grid they can be allocated PRBs in during allocation process. If the UE is a CC-UE, it can be allocated PRBs in the common area by restricting allocation of PRBs in the CE-UE area. If the UE is a CE-UE, it can be allocated PRBs in the CE-UE area in the cell they belong to by restricting allocation of PRBs in the common area. If a UE, independent of the classification, needs to send control information, e.g. SR, they will be allocated PRBs in the PUCCH area. The size of the PUCCH area was configured depending on the total number of UEs in the network so that the UEs would have enough PRBs to transmit SR, Channel Quality Information (CQI) reports and ACK/NACK. How the different areas are restricted can be seen in Figure 4.1.

4.3.1 Results from Static Approach

The outage for static coordination can be seen in Figure 4.6. The static coordination is optimized for 450 UEs.

A utilization of the PRB grid can be seen in Figure 4.7. The plot shows utilization for the PRBs available for allocation for UEs, the PRBs for PUCCH are excluded.

The number of PRBs allocated for CE-UE can be depicted in Figure 4.8. The plot shows the mean number and the highest allocation of PRB for each UE.

The outage in Figure 4.6 was above the reliability requirement of 99.9 % due to CE-UE being allocated more than two PRBs as Figure 4.8 shows. This indicated that further improvements could be done to the static coordination method. The continued investigation of said method will be detailed in the next section.

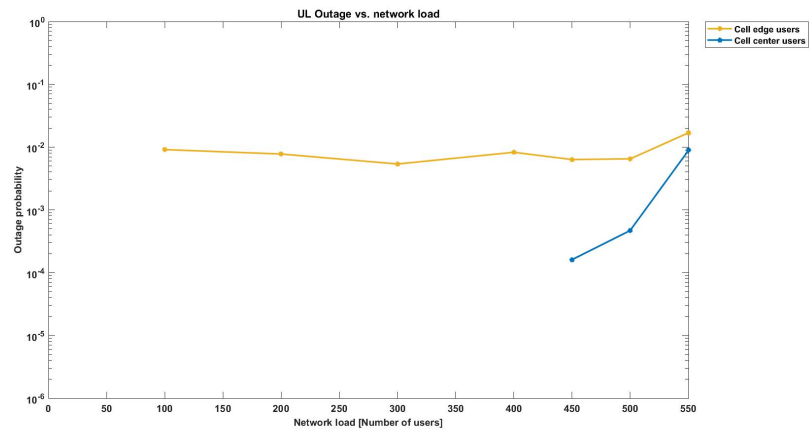


Figure 4.6: Outage for CE-UE and CC-UE, for different network loads.

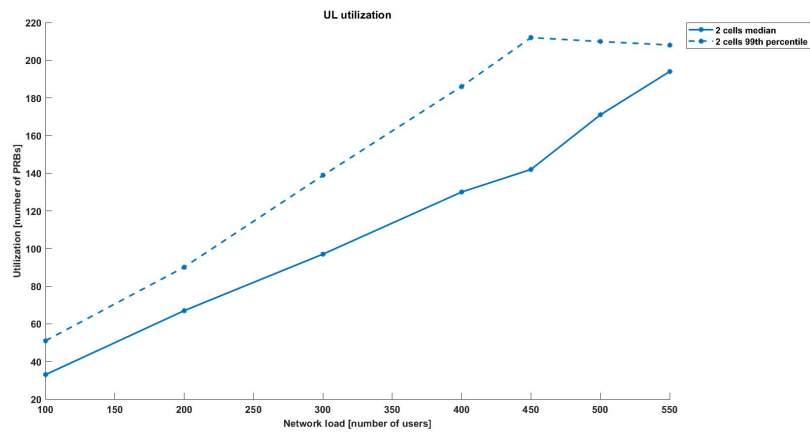


Figure 4.7: Mean and 99th percentile utilization of PRB Grid for different network loads.

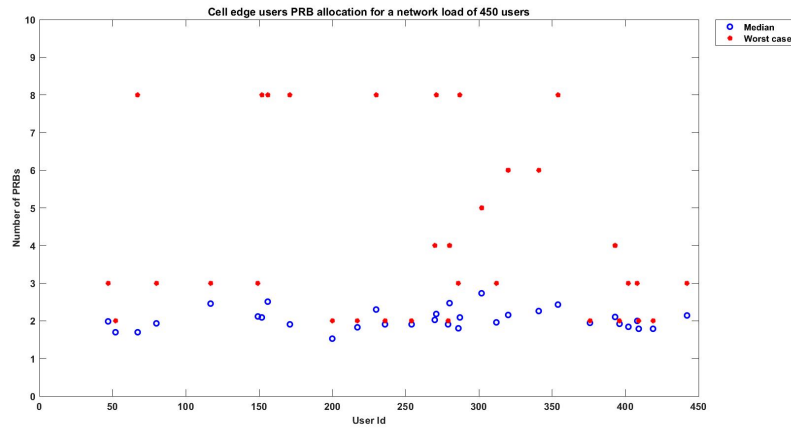


Figure 4.8: Number of PRB allocated per uplink slot for CE-UE.

4.4 The Static Coordination Method, Second Iteration

The first approach at static coordination showed that further improvements could be made regarding the number of PRBs allocated to CE-UEs. When UL SINR for CC-UE and CE-UE, Figure 4.9 and 4.10, were compared, it was shown that CC-UE and CE-UE had similar UL SINR. CE-UEs are transmitting on restricted area with no interference i.e. the UL SINR should be higher for CE-UEs than for CC-UEs. The SINR plots indicated that both the LA process as well as the allocation process needed to be investigated in depth. The investigation showed that the LA estimated a low SINR for CE-UE.

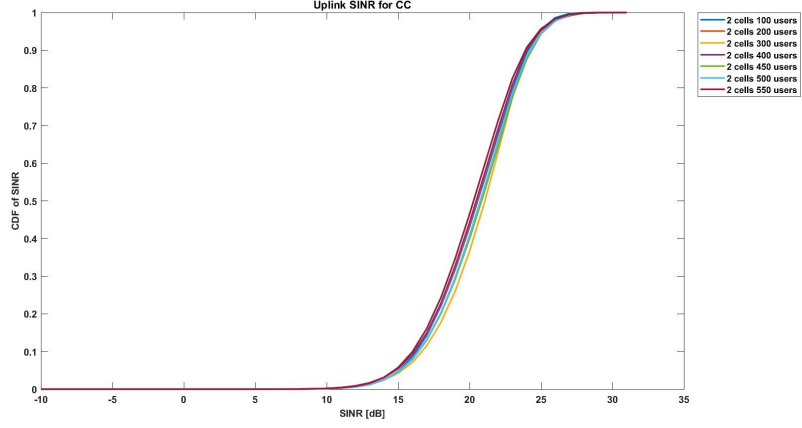


Figure 4.9: SINR for CC-UE with different network loads. From the first implementation of static coordination method.

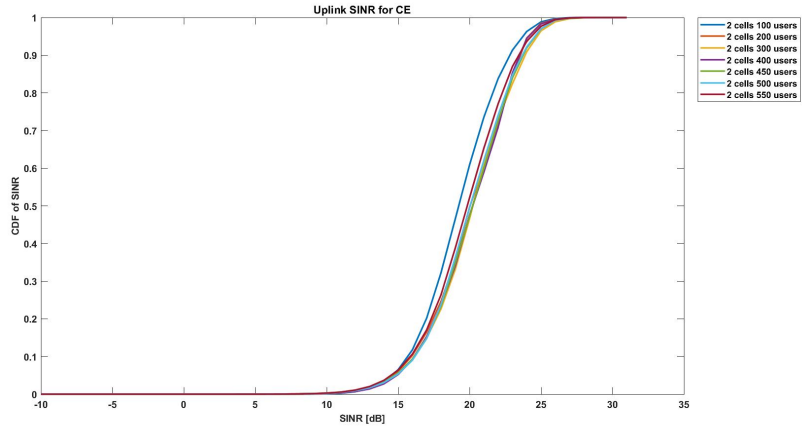


Figure 4.10: SINR for CE-UE with different network loads. From the first implementation of static coordination method.

4.4.1 Increasing the SINR

The reason for the SINR not increasing as much as was assumed was due to the SINR target for the UE transmit power control that was set to 10 dB. Since CE-UE were transmitting in a restricted area, the SINR target was unnecessarily low, since there were no other UEs transmitting on the same PRBs. A proposed solution to increase the SINR was to increase the transmit power for CE-UE. Since the interference to the other cell was assumed to be negligible, the LA margin could be set to 0 dB for CE-UEs. The power control was manipulated to always choose P_{Max} (24 dBm) in equation (2.3) for CE-UEs.

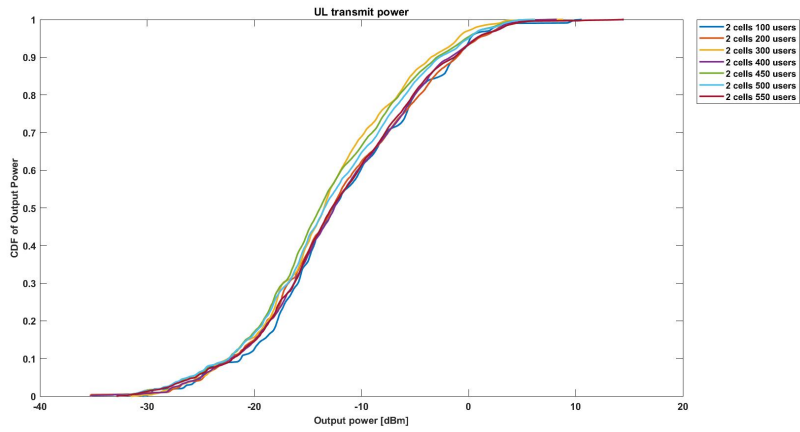


Figure 4.11: UL transmit power before power control modifications.

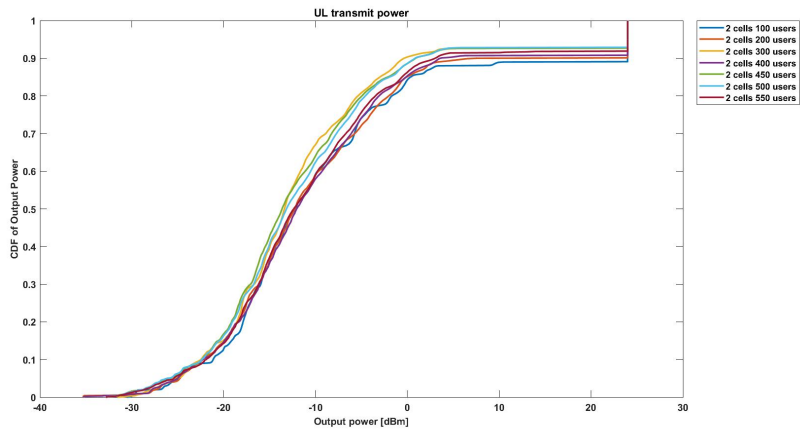


Figure 4.12: UL transmit power after power control modifications.

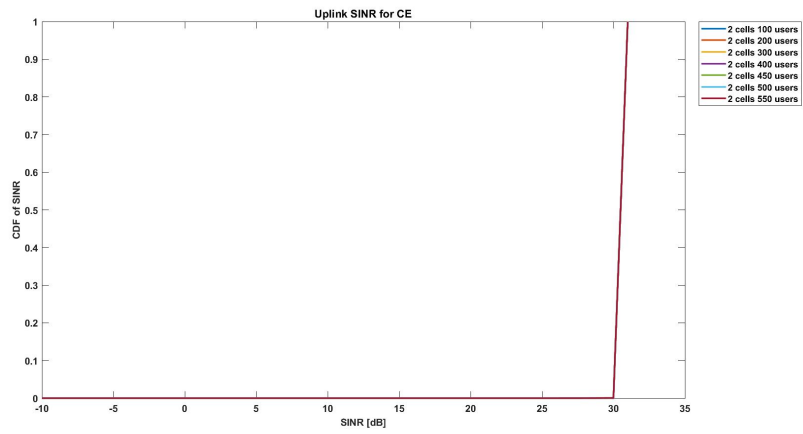


Figure 4.13: UL SINR for CE-UE.

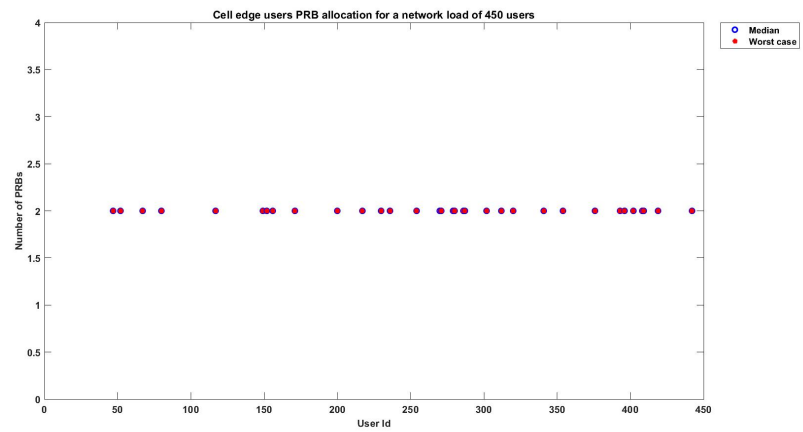


Figure 4.14: The highest and mean number of PRB allocated for CE-UE.

Table 4.3: Parameters for static allocation method, second iteration.

| | |
|----------------------------------|--------------------|
| RSRP threshold | 3 dB |
| CE-UEs in cell 0 | 11 UEs |
| CE-UEs in cell 1 | 22 UEs |
| Size of protected area in cell 0 | 8 PRBs |
| Size of protected area in cell 1 | 16 PRBs |
| Transmit power for CE-UE | P_{Max} (24 dBm) |
| LA Margin for CE-UE | 0 dB |

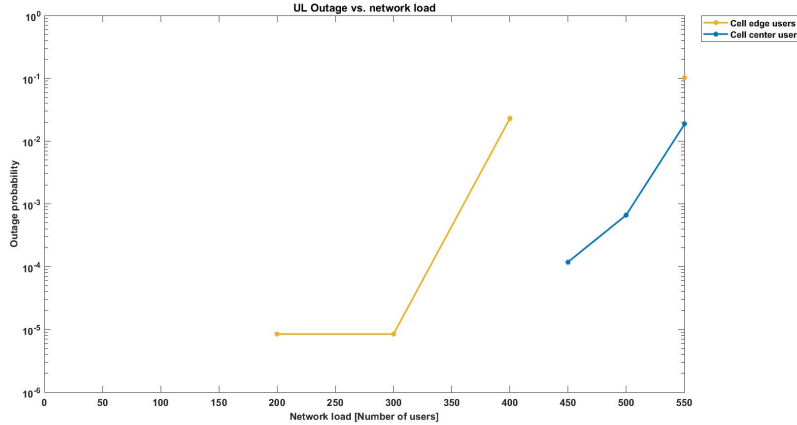
4.4.2 Results

The increase in UL transmit power, due to the power control modification, can be seen by comparing Figures 4.11 and 4.12.

The increase in transmit power for CE-UE has also increased the UL SINR, depicted in Figure 4.13.

In Figure 4.14 it can be seen that, with this modification, CE-UE were never allocated more than 2 PRBs.

The outage for CE-UE, with power control modifications, can be seen in Figure 4.15.

**Figure 4.15:** UL outage with power control modifications.

The drawback with static coordination is that it cannot handle variations in the network system, and this is the reason behind the next approach, dynamic coordination. With the static approach, the same number of PRBs restricted for CE-UEs is the same for all UL slots, although the number of CE-UEs that have data to transmit might vary between UL slots.

4.5 The Dynamic Approach

A drawback with static allocation that was discovered early was that the static coordination had to be optimized for a specific network load. To further improve the coordination method, a dynamic coordination method was proposed. Said method would dynamically alter the sizes of the restricted areas for each UL slot, depending on the number of CE-UEs that were to transmit. The different steps needed to implement the dynamic coordination method and the results it yielded are detailed in the sections below. The implementation of dynamic coordination is a further development from the previous implementation.

4.5.1 Size of the Restrictions

For the restricted area sizes to change dynamically, the number of CE-UEs in each slot and cell had to be calculated. This was solved by adding a feature that iterated over the buffer, were all UEs that have sent an SR, are stored. Figure 4.14 showed that CE-UE were allocated 2 PRBs, which meant that the sizes of the restrictions were set to be two times larger than the number of CE-UEs that had data to transmit per UL slot.

4.5.2 Interference Filter

A consequence with the sizes of the restrictions changing every UL slot, was that the estimated SINR became impaired for PRBs changing from being restricted to not being restricted, or vice versa. For example, a PRB used in the restricted area would not have any interference, however, if that PRB were allocated to a CC-UE in the next UL slot, it would be exposed to interference. This caused the SINR estimation to be inaccurate as it would estimate a low interference when the actual transmission would be exposed to interference. This problem was solved by implementing two changes in simulator B. The first change was to the interference filter. It was altered to only be updated when a PRB was used by CC-UEs. The second change regarded interference for CE-UEs. Instead of using the interference stored in the filter, a minimum interference, set by the simulator, was used for the SINR estimation.

Table 4.4: Parameters for dynamic allocation method.

| | |
|-----------------------------------|--------------------|
| RSRP threshold | 3 dB |
| CE-UEs in cell 0 | 11 UEs |
| CE-UEs in cell 1 | 22 UEs |
| Size of restricted area in cell 0 | Dynamic |
| Size of restricted area in cell 1 | Dynamic |
| Transmit power for CE-UE | P_{Max} (24 dBm) |
| LA Margin for CE-UE | 0 dB |

4.5.3 Results

Figure 4.16 shows the outage curve with the dynamic coordination.

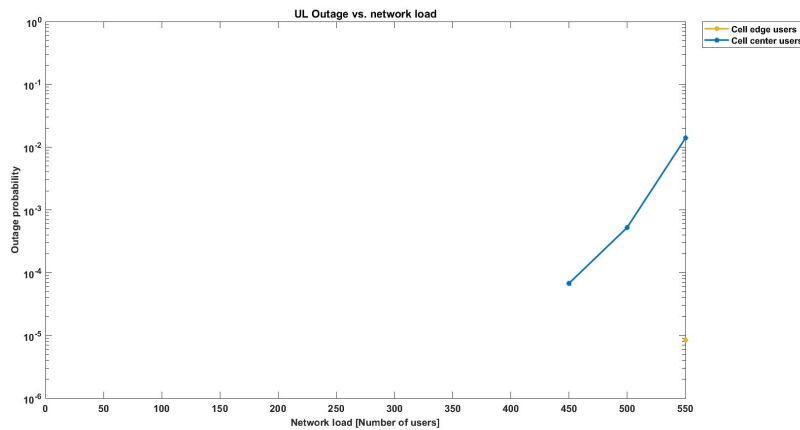


Figure 4.16: Outage for the worst case user with dynamic allocation.

A utilization of the PRB grid can be seen in Figure 4.17. The plot shows utilization for the PRBs available for allocation for UEs, the PRBs for PUCCH are excluded.

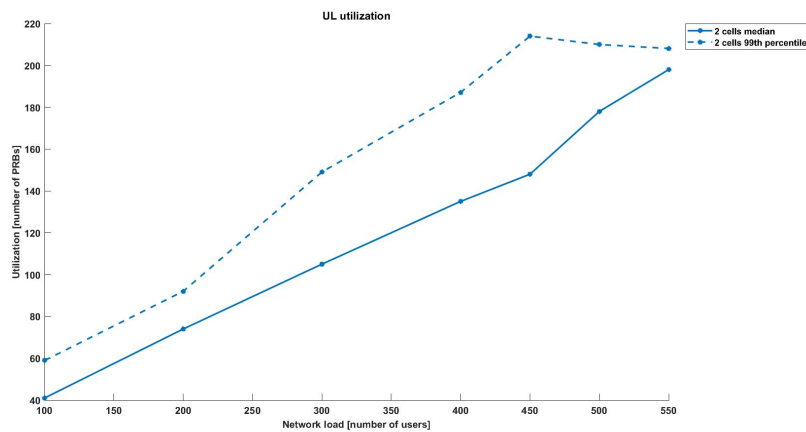


Figure 4.17: Utilization of PRB grid for different network loads with dynamic allocation.

4.5.4 Comparison

The final results from the dynamic coordination will be compared to the baseline, i.e. the results from when no coordination was implemented. The compared

outage probability can be seen in Figure 4.18.

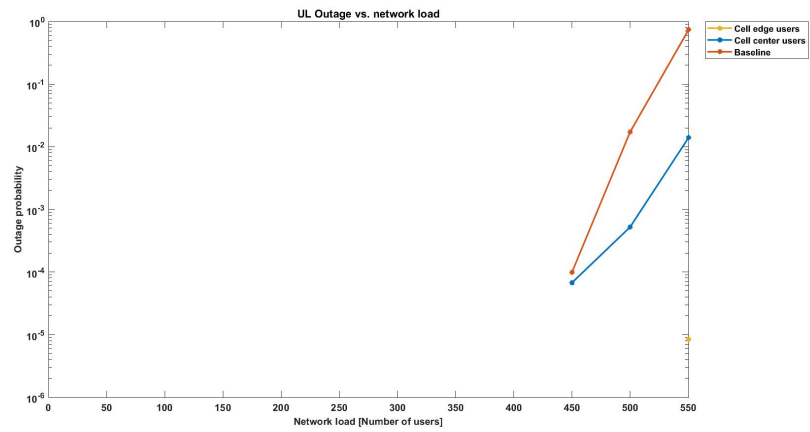


Figure 4.18: Comparison of outage for worst case UEs for dynamic approach and baseline.

Discussion and Conclusion

In this chapter the results from the different coordination methods will be discussed and the thesis will be concluded.

5.1 Static Coordination Method

The static coordination method showed to be inadequate for varying network loads. This is due to the sizes of the restricted areas were fixed, based on a specific network load. The total number of CE-UEs changed unpredictably with the varying network loads as well as their placement. The distribution of CE-UEs between the cells also changed with the network load, which can be seen in appendix A. The static coordination method required that the system needed to be ran beforehand to gather information so that the sizes of the restricted areas could be decided. With this information, the restricted areas were chosen such that there is enough PRBs for the mean number of CE-UEs to be allocated in each UL slot. But there needed to be a margin for the restricted areas when more CE-UEs wanted to transmit, to reduce the probability of UEs being queued. The trade off between choosing a sufficient amount of PRBs to handle all CE-UEs while still keeping the areas as small as possible is what make the static allocation algorithm quite problematic. The cost of restricted areas not being fully allocated is two-fold since the restricted area to one cell is restricted for the other. This can cause a problem in the case where the restricted areas are not fully occupied while the common areas for both cells are, and there are still CC-UEs that want to be scheduled. These CC-UEs will be queued to the next UL slot even though there are available PRBs in the system. Figure 4.15 shows that for the optimized network load, 450 UEs, no outage probability can be seen for CE-UEs, however, at 400 UEs, the outage probability is increased.

In the first approach it can be concluded that coordinating schedulers between cells with a static allocation can improve the reliability for an increased number of users. However the improvement is only for the network load that the static parameters have been optimized for. The improvement is not enough to meet the reliability requirement of 10^{-3} which demonstrates that further improvements need to be done.

5.2 Dynamic Coordination Method

With the dynamic coordination method, the flaws of static coordination were handled by adjusting the sizes of the restricted areas depending on the number of CE-UEs in each UL slot. In Figure 4.18 the end result from the dynamic coordination method is compared to the baseline. The outage for CE-UEs is almost non-existing, which can be explained by them transmitting in a restricted areas where there is no ICI. For CE-UE there is a packet that has exceeded the 10 ms latency requirement, since this packet only occurs in one out of 100000 transmissions, it is hard to explain. An explanation is that the simulator has a random generator to decide if a received packet is in error. A random number is drawn and compared to a BLER calculated based on the received SINR and MCS used for the packet. An explanation of why an error was generated for a CE-UE for this particular case may be that the model for BLER v.s. SINR/MCS may have low but non-zero minimum value which may have generated a single error across all the 100000 packets simulated for this load-point.

The utilization of PRBs, depicted in Figure 4.17, shows that the 99th percentile has been lowered for lower network loads and the median has been lowered for higher network loads compared to no coordination that can be seen in appendix B. Even though the median has been lowered for a high network loads it is still high and is approaching the 99th percentile, which could explain the outage probability for CC-UEs. The number of PRB allocated for CC-UE is another explanation for the outage probability. It can be seen in appendix C that CC-UE are, in worst case, allocated over 25 PRBs.

5.3 Conclusion

In the scope of this thesis was to investigate if the network capacity could be increased while maintaining the reliability requirement of 99.9 % by coordination of schedulers.

The static coordination method had major flaws and proved to be an insufficient coordination method. However the implementation of the method was helpful to gain understanding of the system and became the basis for the dynamic coordination method.

The investigation showed that with a dynamic coordination of schedulers the capacity could be increased from 450 UEs to 500 UEs (10% capacity increase), while maintaining the reliability requirement.

In conclusion, a gain in network capacity can be made by coordination of schedulers. However, further investigation into different methods and parameters related to classifying CE-UEs can be done to conclude if the coordination can be further improved.

References

- [1] Meryem Simsek, Adnan Aijaz, Mischa Dohler, Joachim Sachs, Gerhard Fettweis, *5G-enabled tactile internet* IEEE Journal of Selected Areas in Communications, vol. 34 , no. 3, pp. 460-473, Nov. 2016.
- [2] Ericsson Reaserch, ABI <https://www.ericsson.com/en/blog/2019/11/unlock-the-value-on-industry-4-0>
- [3] Ericsson, *Boosting smart manufacturing with 5G wireless connectivity*, Feb, 2019. Accessed on: May 26, 2020. [Online]. Available: <https://www.ericsson.com/en/reports-and-papers/ericsson-technology-review/articles/boosting-smart-manufacturing-with-5g-wireless-connectivity>
- [4] E. Dahlman, S. Parkvall, J. Sköld, *5G NR: The Next Generation Wireless Access Technology*. London: Elsevier, 2018.
- [5] Zexian Li, Hamidreza Shariatmadari, Bikramjit Singh, Mikko A. Uusitalo, *5G URLLC: Design Challenges and System Concepts*, 2018 15th International Symposium on Wireless Communication Systems (ISWCS), Lisbon, 2018.
- [6] 3GPP, *NR; User Equipment (UE) radio transmission and reception; Part 1: Range 1 Standalone*, technical specification (TS) 38.101, March 2020.
- [7] 3GPP, *Service requirements for the 5G system*, technical specification (TS) 22.261, June 2017.
- [8] Osama Al-Saadeh, Kimmo Hiltunen, Kittipong Kittichokechai, Alexey Shapinz, Majid Geramix, Henrik Asplund, Eric Wang, Gustav Wikström, Joachim Sachs. *5G Ultra-Reliable Low-Latency Communication for Factory Automation at Millimetre Wave Bands*
- [9] Haenggi, Martin & Andrews, Jeffrey & Baccelli, François & Dousse, Olivier & Franceschetti, M.. (2009). *Stochastic Geometry and Random Graphs for the Analysis and Design of Wireless Networks*. Selected Areas in Communications, IEEE Journal on. 27. 1029 - 1046. 10.1109/JSAC.2009.090902.
- [10] 3GPP, *NR; Physical channels and modulation*, technical specification (TS) 38.211, March 2020.

-
- [11] 3GPP, *NR; Multiplexing and channel coding*, technical specification (TS) 38.212, March 2020.
 - [12] 3GPP, *NR; Physical layer measurements*, technical specification (TS), 38.215, July 2018.
 - [13] 5G ACIA *A 5G Traffic Model for Industrial Use Cases*, White paper, November 2019.
 - [14] 3GPP *Study on channel model for frequencies from 0.5 to 100 GHz*, technical report TR 38.901, January 2018.
 - [15] Knuth: Computers and Typesetting,
<http://www-cs-faculty.stanford.edu/~uno/abcde.html>
 - [16] Ali Zaidi, Fredrik Athley, Jonas Medbo, Ulf Gustavsson, Giuseppe Durisi, Xiaoming Chen. *Chapter 2 - NR Physical Layer: Overview*, 2018 <https://www.sciencedirect.com/topics/computer-science/spectrum-allocation>
 - [17] Ericsson internal

Figures

- [18] Ericsson internal

UE Locations

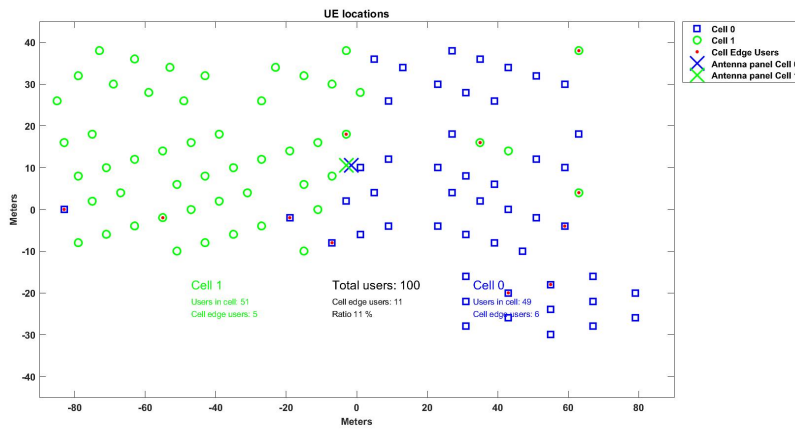


Figure A.1: UE locations for a network load of 100 UEs.

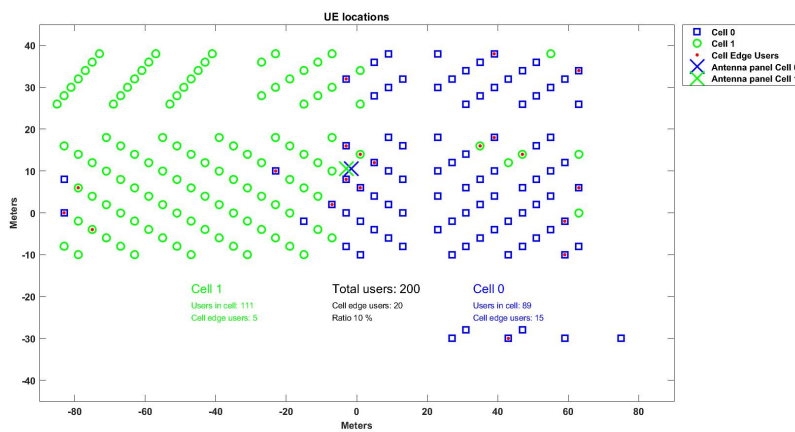


Figure A.2: UE locations for a network load of 200 UEs.

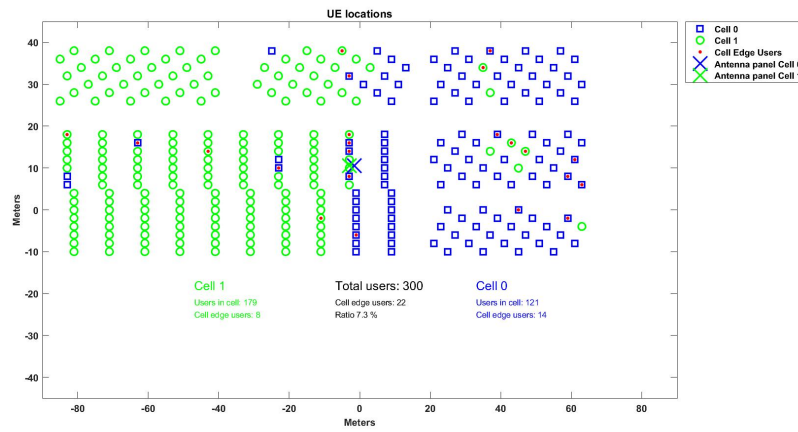


Figure A.3: UE locations for a network load of 300 UEs.

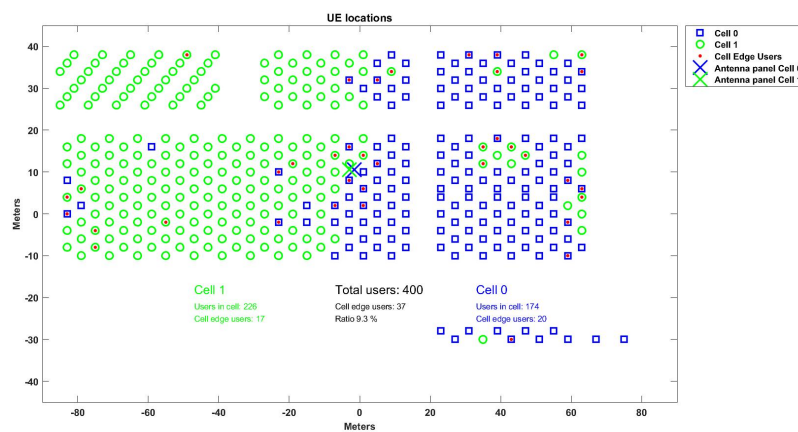


Figure A.4: UE locations for a network load of 400 UEs.

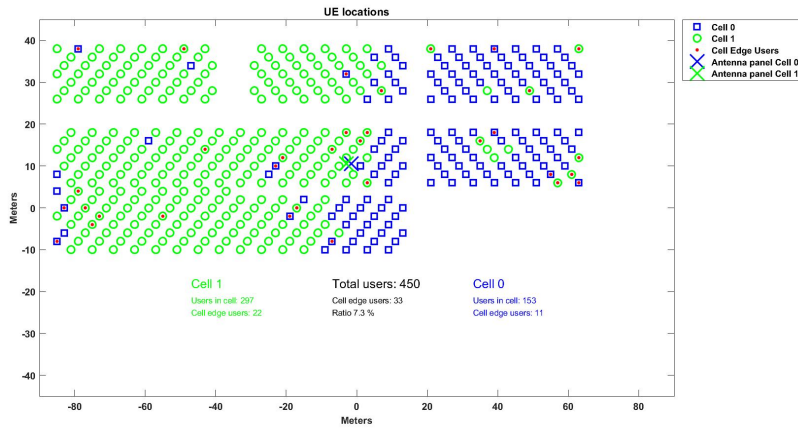


Figure A.5: UE locations for a network load of 450 UEs.

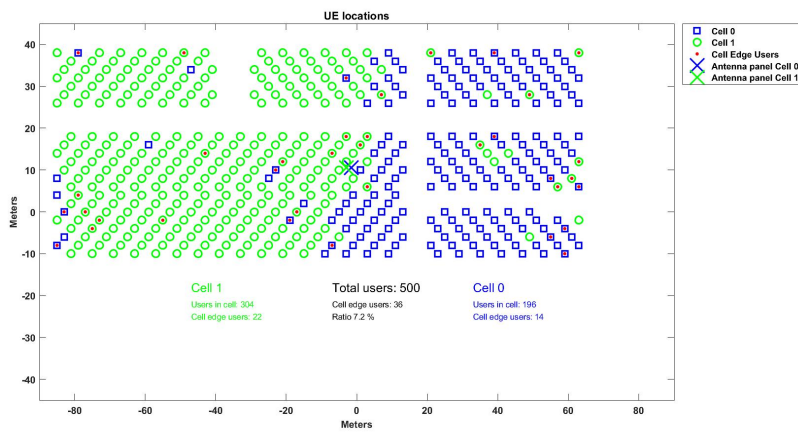


Figure A.6: UE locations for a network load of 500 UEs.

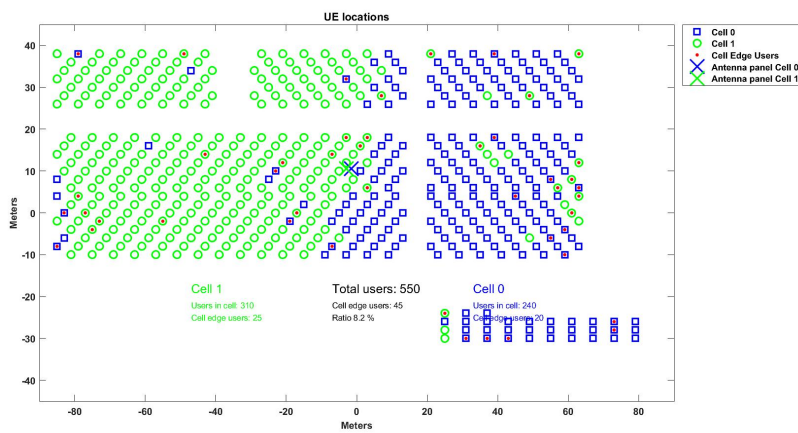


Figure A.7: UE locations for a network load of 550 UEs.

Utilization of PRB Grid For Baseline

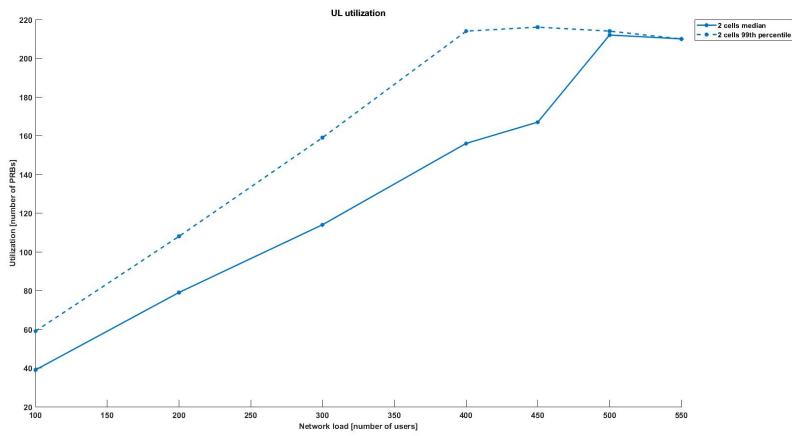


Figure B.1: Utilization of PRB grid for different network loads with no coordination (baseline).

PRB Allocation For CC-UE

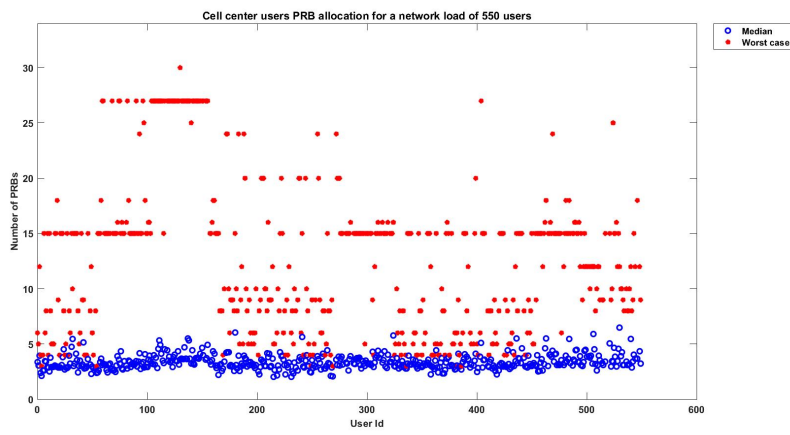


Figure C.1: Mean and worst case PRB allocation for CC-UEs at a network load of 550 UEs.

Data Traffic Arrival Pattern

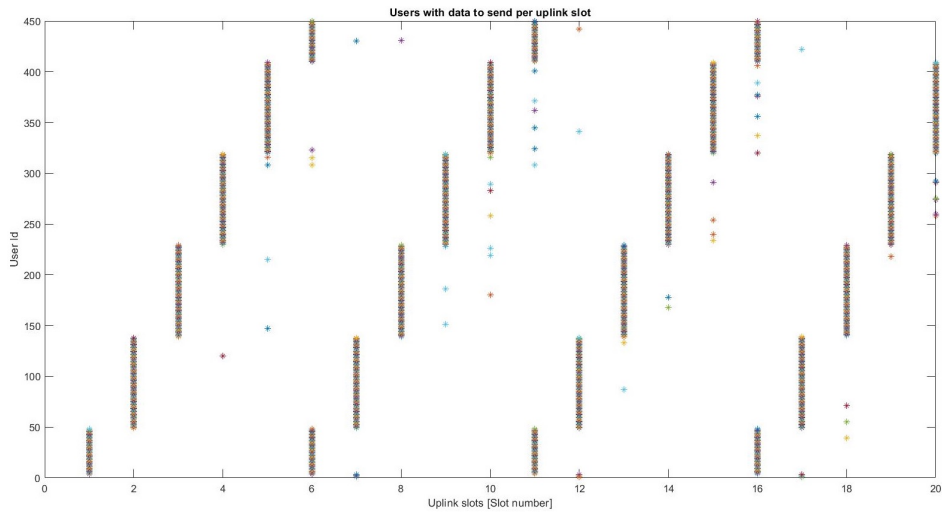


Figure D.1: Data traffic arrival pattern for 20 uplink slots.



LUND
UNIVERSITY

Series of Master's theses
Department of Electrical and Information Technology
LU/LTH-EIT 2020-775
<http://www.eit.lth.se>